

International Journal of Heat and Technology

Vol. 43, No. 5, October, 2025, pp. 1749-1756

Journal homepage: http://iieta.org/journals/ijht

Control of V-Shaped Channel Angle Contains Three Hot Obstacles

Check for updates

Mustafa Salah Rahomey^{1*0}, Isam Mejbel Abed¹⁰, Nejla Mahjoub Said²⁰

- ¹ Mechanical Engineering Department, College of Engineering, University of Babylon, Babylon 51001, Iraq
- ² Department of Physics, College of Science, King Khalid University, Abha 61413, Saudi Arabia

Corresponding Author Email: mahjoub nejla@yahoo.fr

Copyright: ©2025 The authors. This article is published by IIETA and is licensed under the CC BY 4.0 license (http://creativecommons.org/licenses/by/4.0/).

https://doi.org/10.18280/ijht.430513

Received: 7 July 2025 Revised: 5 October 2025 Accepted: 17 October 2025 Available online: 31 October 2025

Keywords:

hot obstacle, channel, heat exchanger, different shape channel, Galerkin method

ABSTRACT

This paper presents a numerical analysis using COMSOL version 6.2 to study heat transfer by forced convection (F.C) within a channel containing a nanofluid/water, with three concentric hot obstacles. The flow is assumed to be laminar, and the surfaces of hot obstacles are assumed to be heated at a certain constant temperature (Th), while the upper and lower channel walls are assumed to be cooled to another constant temperature (Tc). The momentum equations are solved numerically using the finite element technique, specifically the Galerkin method. The fluid flow and heat transfer characteristics were analyzed across a range of variables, including Reynolds number values ranging (10-500), the channel angle (180°-60°), and the volume fraction (0-0.1), respectively. The results showed that the channel slope contributes to improving the velocity distribution, flow lines, and temperature behind the heated cylinders, especially at high Reynolds numbers, and that the best improvement in the modified Nusselt number is achieved when the channel walls are angled at right angles. This result is of great importance in developing more efficient and less expensive industrial heat exchangers. The new V-shaped design appears to pave the way for a new generation of heat exchangers.

1. INTRODUCTION

Many significant industrial processes, such as those in solar energy collectors, chemical reactor stimulation, and model power plants, are idealized by the flow of fluids via a system of cylinders [1]. One but, in the construction of supporting structures, for example, these forced flows also serve as an idealization of many flows of industrial significance, like the flow of tubular heat exchangers [2]. As a result, numerous studies have been conducted over the years to analyze the heat and momentum transfer characteristics of cylinders with various cross-sectional shapes [3-5]. In this context, Harimi et al. [6] studied the F.C heat transfer and fluid flow behavior within a channel containing a hot obstacle equipped with three control rods, using the grid-net method in their analysis. Their study was based on a Re = 200 and Pr = 0.7 and 7.0. When compared to a single cylinder, they discovered that the master cylinder's average Nusselt number steadily drops. This finding is particularly obvious for lower cylinder spacing ratios because the master cylinder's heat transmission rate is much different from that of tiny rods. Chakraborty and colleagues performed a numerical study on a hot obstacle placed inside a flat rectangular channel [7]. The researchers conducted estimates for blockage ratios (1.54 and 2.0) and for varying Reynolds numbers (0.1 and 200). The researchers discovered that as the Re number increases, so does the separation angle with the recirculation zone's length. Additionally, Paramane et al. [8] used the heat transfer due to F.C around a hot obstacle rotating at parameter ranges Re = 20 to 160, and Pr = 0.7. The average Nusselt number, according to the researchers, rises with rising Re and falls with increasing rotation rate until reaching a practically constant value at the greatest rotation rate for all Re. The F.C for Al₂O₃ nanofluid passing via a channel was examined by Aminossadati et al. [9]. According to the researchers' findings, the microchannel transfers heat more effectively at higher Reynolds numbers. Furthermore, the researchers found that increasing the volume fraction of the solid material in turn leads to a higher average Nusselt number. At higher Re number values, the pace of this growth is much larger. However, Singha and Sinhamahapatra [10] simulated flow around a hot obstacle placed in the centre of a channel using the finite volume approach. The normalised channel height range (2-8), and the researchers used Reynolds numbers of 45, 100, 150, and 200. At a flow Reynolds value of 100, the researchers noticed the presence of vortices. The Reynolds value is a criterion for determining the critical gap size, especially if the standard gap between the cylinder and the solid wall is less than about 1.0. Additionally, Rahim Mashaei et al. [11] studied the effect of laminar convection of a nanofluid composed of aluminum oxide and water within a flow channel containing independent heat sources, using numerical simulation methods to analyze the phenomenon. In order to facilitate energy exchange between the nanofluid and the heat sources, the bottom wall of the channel had to be heated while the other channel surfaces were maintained at a constant temperature. The researchers used a Reynolds number (Re) range of 50, 100, 200, 400, and 1000, and a particle size ratio (φ) of 0 in pure water, 1%, and 4%. An irregular velocity symmetrical throughout the channel height may be produced by using nanofluids. According to the researchers' findings, the mean Nu number increased by up to 38% for every example they looked at when compared to the base fluid. In order to investigate the impact of an oscillating cylinder on heat transfer.

From hot masses in a channel flow, Fu and Tong [12] also performed numerical simulations. The flow and temperature fields were described by the researchers using the Lagrange-Eulerian kinetic description approach. They investigated how the hot wall's heat transmission characteristics were impacted by Reynolds number, oscillation frequency, and oscillation amplitude. Their findings showed that when the cylinder oscillation frequency is in the lock zone, heat transmission from the hot masses is greatly increased. In contrast, Salimevendegila and Öztop [13] employed the finite element technique to perform a numerical simulation of F.C of water and nanofluids as they flow around hot obstacles within a channel. To analyze the effect of variables on the fluid flow and convective heat transfer processes, the study focused on several factors, including different parameters, for example, (Re = 100 to 1000), (φ = 0 to 0.04), and (the distance of the hot obstacles = 0.5 to 8). They discovered that at the maximum Reynolds number values for hot obstacles, the average Nusselt number rises by around 20%. Mohebbi et al. [14] also used three distinct nanofluids to mimic F.C in an extended-surface channel using a two-dimensional lattice Boltzmann approach. The researchers discovered that the copper oxide nanoparticlecontaining nanofluid enhanced heat transfer more effectively than the titanium dioxide and water, and aluminium oxide and water nanofluids. Zhang et al. [15] also investigated the flow of a hot obstacle that was elastically constructed and had a separator plate connected under laminar flow conditions with a Re = 100. They solved the governing equations for 2D incompressible fluids using a finite volume model.

Al-Sumaily et al. [16] used the finite element approach to investigate F.C heat transfer from a single hot obstacle containing a porous medium (PM). According to the researchers' findings, the PM greatly improves heat conduction and lessens the wake behind the cylinder. In order to determine how PM affects the rate of heat transmission, Rashidi et al. [17] also carried out convective heat transfer within a P.M. heat exchanger. Various Reynolds values and thicknesses of dimensionless P.M. were simulated. At d = 1/3– 1 and Da = 0.01, the researchers discovered that the Nusselt number increased by almost 96% as the thickness of the PM increased. Matin and Pop [18] investigated heat and mass transmission by fully developed F.C in a horizontal porous tube containing a nanofluid. The researchers made the assumption that a constant heat flow was present in the channel walls. They examined the impacts of nanoparticle size ratio, Darcy numbers, and Brinkman numbers on the distributions of temperature, velocity, and Nusselt number using the Brinkman model for flow in PM. The researchers came to the conclusion that raising the Darcy number causes the Nusselt number and the concentration of dimensionless nanoparticles to rise as well. However, a computational examination of the impact of PM on F.C around a compact hot obstacle was reported by Al-Sumaily et al. [19]. The cylinderto-particle diameter ratio was used by the researchers throughout a broad range of Reynolds numbers, ranging from 1 to 250. In contrast to an empty channel, they found that the presence of PM around the hot cylinder improves total heat transmission and raises the pressure drop. Lastly, the flow and subsequent heat transmission in a channel with a heated cylinder were examined by Al-Sumaily and Thompson [20]. While maintaining the structural characteristics of the PM constant, they used suitable dimensionless number ranges, such as (Re = 1 to 250) and (kr = 0.1 to 100). They came to the conclusion that steady wakes would be produced in the empty channel by raising the Reynolds number. The researchers came to the conclusion that, in the case of the channel filled with PM, the damping produced by the PM would result in very steady, prolonged flows in the areas ahead and behind the cylinder. Based on a comprehensive review and thorough knowledge of the latest developments, it was found that most previous work focused on flat, porous, wavy, or heterogeneous channels. In contrast, studies on V-shaped channels were very scarce; the current investigation involves a two-dimensional computational study of F.C heat transfer in a V-shaped channel featuring multiple heated obstacles.

2. MATHEMATICAL MODEL

A numerical study was conducted to analyze the thermal behavior of three heated obstacles placed inside a V-shaped channel. The detailed geometric configuration is shown in Figure 1. The diameter of each cylinder is D, while the left and right parts of the channel extend 12D in length and form an acute angle α . The channel width (t) and the distance between the cylinder centers (S) extend to 4D and 6D, respectively. The upper and lower channel walls maintain a cool, constant temperature, Tc, while the inner cylinders are exposed to a uniform, elevated temperature, T_h .

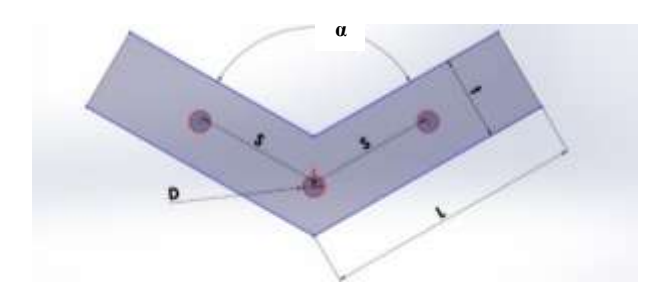


Figure 1. The physical field and the generally adopted coordinate system

The analysis assumes a steady, two-dimensional, laminar, and incompressible flow regime. All solid boundaries, including the channel and cylinder surfaces, satisfy the no-slip condition and are treated as impermeable. In contrast, the inlet, outlet, and the interface between the two channel sections allow fluid passage and are therefore considered permeable boundaries. Therefore, the continuity, momentum and energy equations in the dimensionless form for the present work are given by:

Continuity equation:

$$\frac{\partial U_{conv.}}{\partial X} + \frac{\partial V_{conv.}}{\partial Y} = 0$$

Momentum equation:

$$\begin{array}{c} U_{conv.} \frac{\partial U_{conv.}}{\partial X} + V_{conv.} \frac{\partial U_{conv.}}{\partial Y} = -\frac{\partial P}{\partial X} + \frac{1}{Re} \bigg(\frac{\partial^2 U_{fluid}}{\partial X^2} + \frac{\partial^2 U_{fluid}}{\partial Y^2} \bigg) \end{array}$$

$$U_{conv.} \frac{\partial V_{conv.}}{\partial X} + V_{conv.} \frac{\partial V_{conv.}}{\partial Y} = -\frac{\partial P}{\partial Y} + \frac{1}{R_P} \left(\frac{\partial^2 V_{conv.}}{\partial X^2} + \frac{\partial^2 V_{conv.}}{\partial Y^2} \right)$$

Energy equation:

$$U_{conv.} \frac{\partial \theta_{conv.}}{\partial X} + V_{conv.} \frac{\partial \theta_{conv.}}{\partial Y} = \left(\frac{\partial^2 \theta_{conv.}}{\partial X^2} + \frac{\partial^2 \theta_{conv.}}{\partial Y^2}\right) * (Re \text{ Pr})^{-1}$$

2.1 Dimensionless boundary conditions

The dimensionless boundary conditions applied in this study are defined as follows:

Along the upper and lower channel walls as well as the surfaces of the cylinders, the dimensionless velocity components are set to zero, indicating a no-slip condition. These boundaries are also maintained at a constant cold temperature. Hence,

$$U = V = \theta = 0$$

The surfaces of the hot obstacles are kept at a uniform hot temperature, represented in dimensionless form as: $\theta = 1$.

At the interface line between the two regions, continuity conditions are imposed for temperature, stream function, velocity components, and pressure. These ensure smooth transfer of flow and thermal variables across the interface, and are expressed as:

$$\theta = \theta_{nf} \frac{\partial \theta}{\partial X} = \frac{\partial \theta_{nf}}{\partial X}$$

$$\psi = \psi_{nf} \frac{\partial \psi}{\partial X} = \frac{\partial \psi_{nf}}{\partial X}$$

$$U = U_n \frac{\partial U}{\partial X} = \frac{\partial U_{nf}}{\partial X}$$

$$V = V_{nf} \frac{\partial V}{\partial X} = \frac{\partial V_{nf}}{\partial X}$$

$$P = P_{nf} \frac{\partial P}{\partial X} = \frac{\partial P_{nf}}{\partial X}$$

2.2 Local and average Nusselt numbers

The local heat transfer rate at the cylinder surface is represented by the Nusselt number (Nu), which quantifies the ratio of convective to conductive heat transfer. It is expressed as:

$$Nu = \frac{h L}{k_f}$$

$$\frac{q_{wall}}{A} = -k \frac{\partial T}{\partial y} \Big|_{wall} = h(T_{wall} - T_c)$$

The subscript (*wall*) refers to the hot wall, where it acts as the left sidewall in cases one and two, while case three is acted by the surface of the cylinder.

The heat-transfer coefficient may be circulated from:

$$h = -\frac{k_{fluid} \left. \frac{\partial T}{\partial y} \right|_h}{(T_h - T_c)}$$

So, the local Nusselt number:

$$Nu = -\frac{k_{fluid} \frac{\partial T}{\partial s} \Big|_{h} l}{(T_{h} - T_{c}) k_{fluid}}$$

The non-dimensional form can be used as follows:

$$Nu = -\frac{\partial \theta}{\partial \acute{n}}$$

So, the mean Nu for a single hot obstacle is:

$$\overline{Nu} = \int_0^1 \frac{\partial \theta}{\partial n} \, dY$$

And for all cylinders are:

$$\overline{Nu}_{cyl.} = \frac{1}{3} \int_{0}^{3} \overline{Nu}$$

3. GRID INDEPENDENT TEST

To achieve both computational efficiency and high accuracy, a study was carried out to determine the minimum number of elements required to reach a mesh-independent solution. Figure 2 illustrates how the mean Nu for all cylinders varies with the number of elements for four different Re (10, 100, 300, and 500). It is shown that the steady state of the Nusselt number was in the range (4000-7000) of the number of elements for all cases.

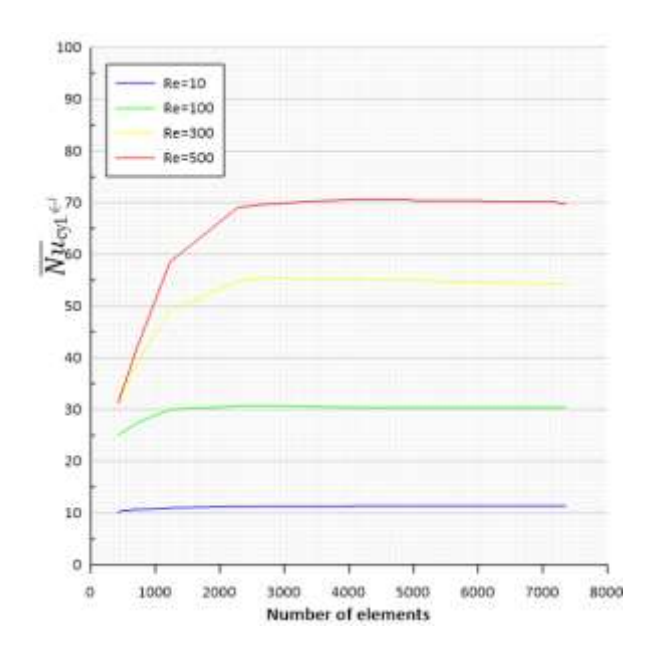


Figure 2. Variation of the mean *Nu* along the perimeter of hot obstacles with the number of elements

4. VALIDATION OF THE RESULTS

This study focuses on F.C heat transfer in the backward-facing step flow caused by a single hot obstacle placed inside a horizontal channel [21]. The properties of Kumar and Dhiman [21] were at Re = 1,200 and Pr = 0.71. the comparison of streamline gives a good agreement between the previous and present results, as shown in Figure 3.

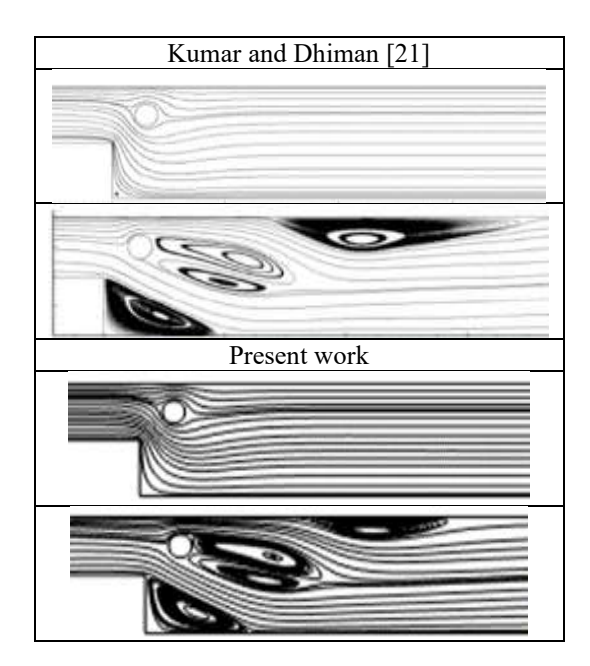


Figure 3. Comparison of streamline profiles from the present study (above) and the results reported by Kumar and Dhiman [21] (below) for Re = 1,200 and Pr = 0.71

5. RESULTS AND DISCUSSION

To understand the temperature and velocity field distribution characteristics of a V-shaped channel, streamlines, isotherms, and the local and mean Nusselt distributions of the channel were considered in several cases. The parameter ranges studied are as follows: $[60 \le \alpha \le 180, 10 \le \text{Re} \le 500,$ and $0 \le \varphi \le 0.1$], respectively. Figure 4 shows the surface velocity and flow lines at various angles to the channel and at (Re = 10). It is noted from the figure that when the angle was 180° (Figure 4(a)), the velocity distribution is uniform in the channel and around the three cylinders. This is normal due to the forced flow mechanism, as the flow encounters the cylinders and is pushed toward the walls. The flow lines will be uniform due to the low inlet velocity (i.e., at a low Reynolds number). When the channel walls are tilted—i.e., the angle between the channel sides is reduced—Figure 4(b)-4(e) will push the velocity over the cylinders, especially the middle one, due to the velocity path, which is often upward. For the surface temperature, Figure 5 under the same conditions as in the previous figure, since the hot obstacles are hot and the channel walls are cold, heat will expand from the cylinders toward the exit (from left to right). The smaller the angle between the two sides of the channel, the closer the heat distribution between the hot cylinders will be observed. This technique will contribute to a more uniform surface heat distribution, especially at low Reynolds numbers.

Moving to high velocity (i.e., at high Reynolds number) (Figure 6), we observed almost zero velocity, with a double vortex forming behind each hot cylinder. This is physically normal, as the high velocity flow will continue toward the exit rather than behind the cylinder. Also, the circular shape of the cylinder will result in less fluid flow behind it. Decreasing the channel angle will result in a more even velocity distribution behind each cylinder, with a reduction in the size of the double vortex. However, another problem arises when the angle decreases. A single, longitudinal vortex appears behind the upper half of the channel (Figure 6(c)-6(e)), increasing in size

as the angle decreases. This can be explained by the fluid flow mechanism, where the channel geometry (especially if the angle is acute) affects the velocity distribution and flow lines.

In general, fluid flow at high speeds around hot cylinders in straight channels leads to premature flow separation. This occurs when the fluid separates from the cylinder surface, creating vortex zones and low-pressure regions behind them. This contributes to increased turbulence and energy loss.

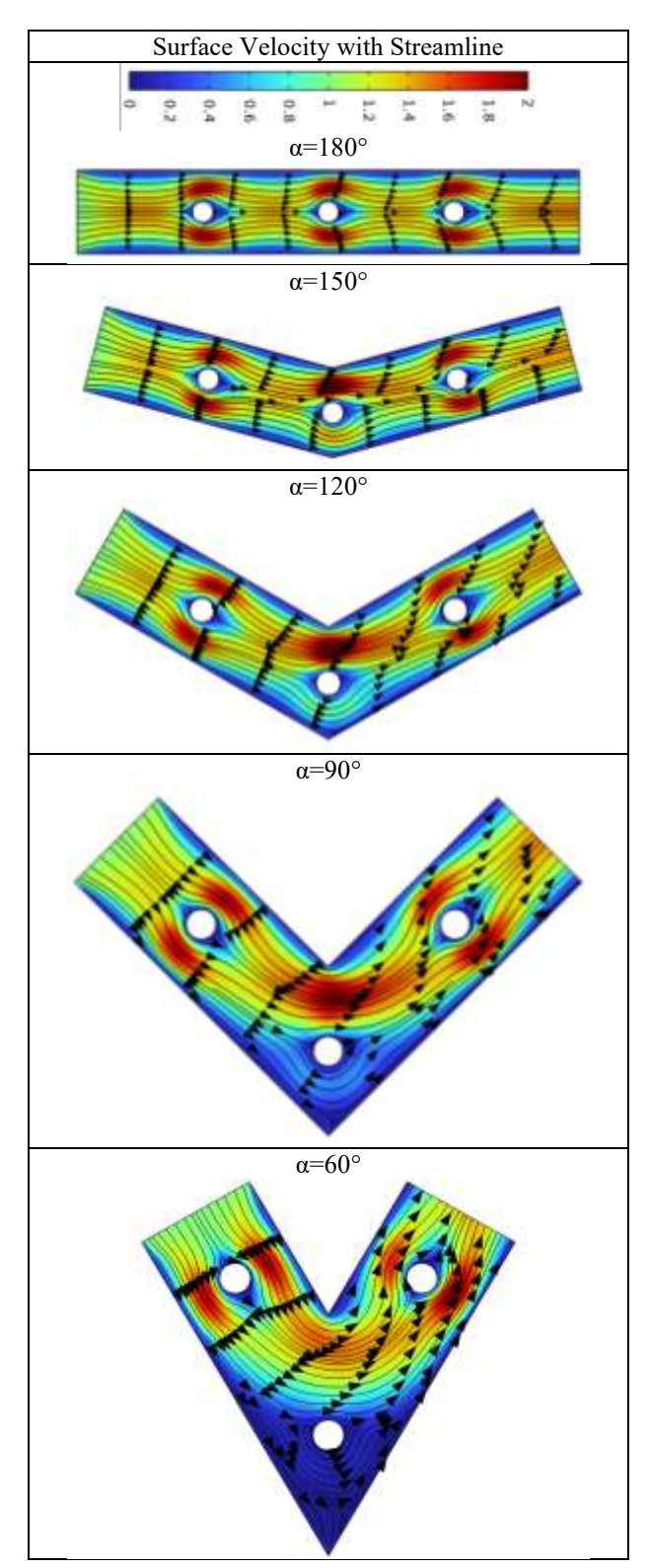


Figure 4. The velocity distribution with streamline at Re = 10 and $\phi = 0.05$ with different channel angle ($\alpha = 180^{\circ}$, 150° , 120° , 90° and 60°) from up to down respectively

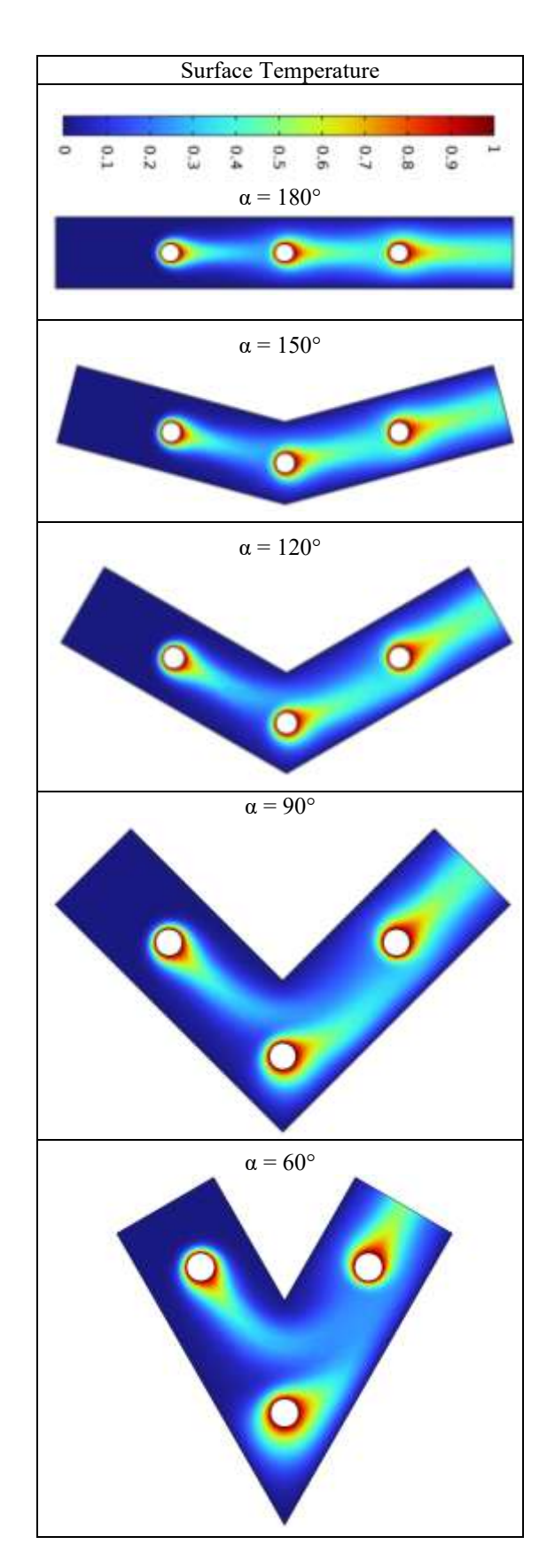


Figure 5. The surface temperature (down) at Re = 10 and ϕ = 0.05 with different channel angle (α = 180°, 150°, 120°, 90° and 60°) from up to down, respectively

To avoid or reduce this, the angle of the channel walls can be reduced, which helps prevent or delay flow separation. This allows the fluid in contact with the surface to remain in flow for a longer period of time, reducing the chances of vortex formation and improving system efficiency.

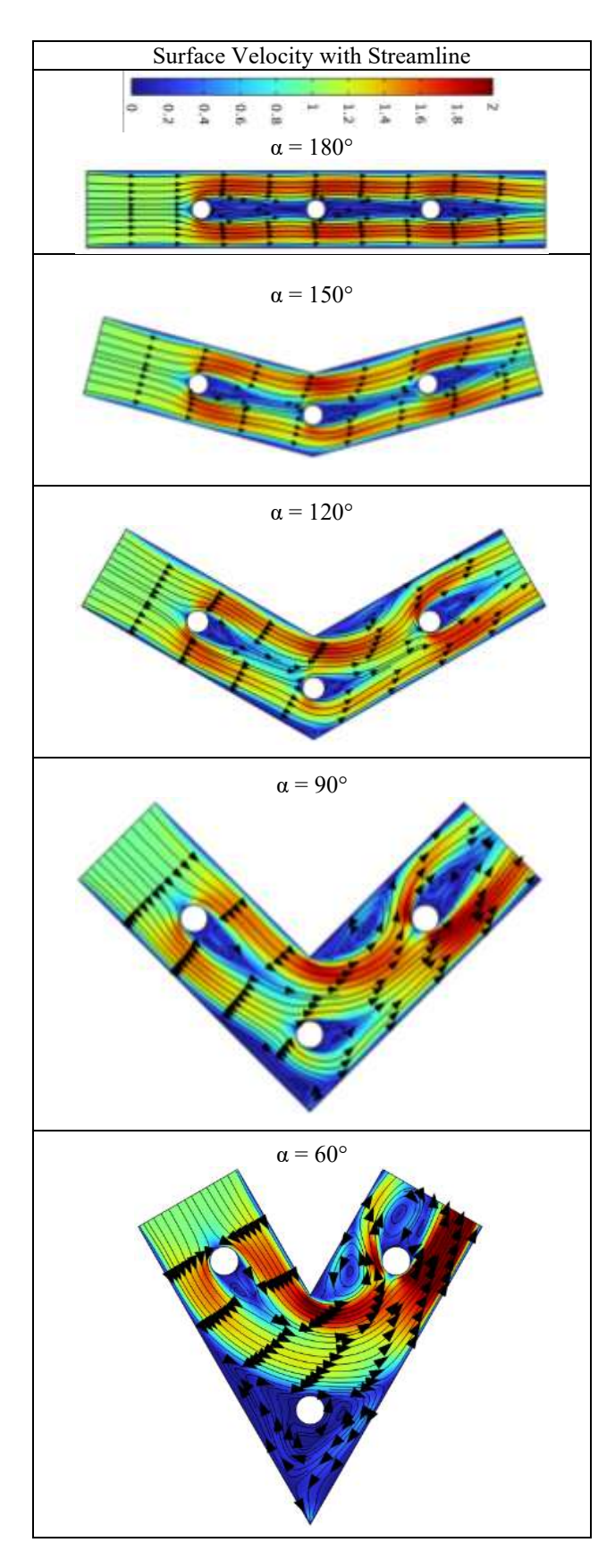


Figure 6. The velocity distribution with streamline at Re = 500 and $\varphi = 0.05$ with different channel angle ($\alpha = 180^{\circ}$, 150° , 120° , 90° and 60°) from up to down, respectively

Regarding the surface temperature, at the same high velocity conditions (Figure 7), a very significant reduction in temperature was observed compared to low velocity. This is due to the high congestion, which leads to the formation of a crescent-shaped shape around each cylinder.

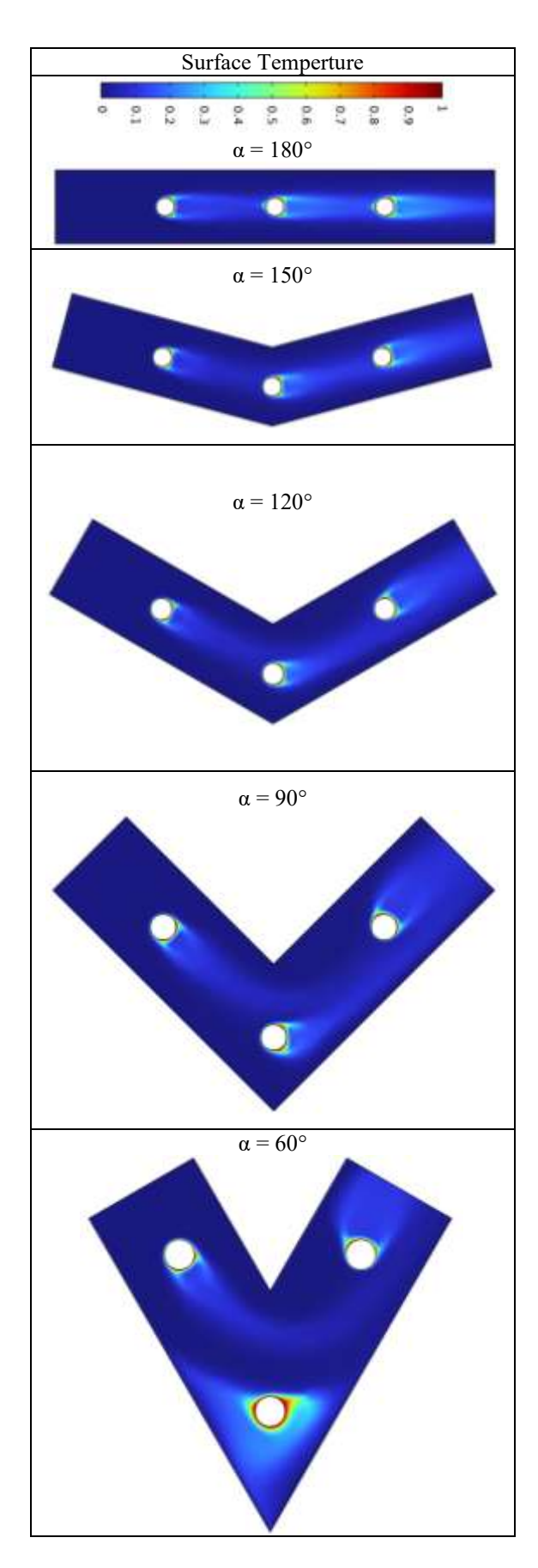


Figure 7. The surface temperature (down) at Re = 500 and φ = 0.05 with different channel angle (α = 180°, 150°, 120°, 90° and 60°) from up to down, respectively

When decreasing the angle of the two sides of the channel, there is no significant change compared to the previous case, except for the last case (Figure 7(a)), where we notice a clear

increase around the middle cylinder. This is due to the flow colliding with the lower corner of the channel, which causes the surface heat to be confined around this cylinder.

To delve further into the channel geometry and the ideal angle for more uniform flow, the heat transfer rate (Nusselt number) for the three hot circular cylinders, calculated from the equation. As is clear from Figure 8, the average Nusselt number increases as the Reynolds number increases for all cases of channel angles. It was also observed that the smallest increase in Nusselt number occurs when the angle is straight (180°).

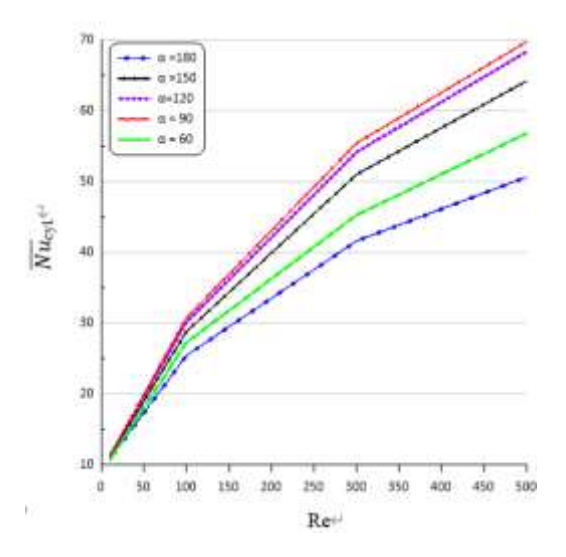


Figure 8. Variation of the mean Nu along the hot surfaces of the hot obstacles with Re for different channel angles

As the angle between the two sides decreases, the Nusselt number for the cylinders increases, respectively, except for the last case (60°), where the Nusselt number decreases below the three cases. As discussed earlier in the velocity and temperature distributions, the flow and heat transfer become more restricted in the final case.

6. CONCLUSIONS

In addition to the fact that the inclined channel occupies a smaller space compared to the straight channel, several conclusions have been drawn based on numerical simulations of forced flow and heat transfer in the channels:

- At a low Reynolds number, the velocity distribution along the streamlines and the surface temperature are uniform for the first case, while the remaining cases are less uniform.
 We conclude that the first case is ideal for low velocities.
- At a high Reynolds number, the surface velocity disappears, forming a double vortex behind the hot circular cylinders, especially in the first case. The smaller the angle between the channel walls, the denser the velocity distribution behind the cylinders will be, with a clear decrease in the size of the double vortex. Therefore, the inclination of the channel (i.e., the inclination of the channel walls) will contribute to improving the velocity and temperature distribution behind the cylinders in the channel.
- We also conclude that the best heat transfer in the channel occurs when the channel walls are right-angled. This was achieved by calculating the modified Nusselt number for hot circular cylinders.

REFERENCES

- [1] Heidary, H., Kermani, M.J. (2010). Effect of nanoparticles on forced convection in sinusoidal-wall channel. International Communications in Heat and Mass Transfer, 37(10): 1520-1527. https://doi.org/10.1016/j.icheatmasstransfer.2010.08.01
- [2] Sahu, A.K., Chhabra, R.P., Eswaran, V. (2009). Effects of Reynolds and Prandtl numbers on heat transfer from a square cylinder in the unsteady flow regime. International Journal of Heat and Mass Transfer, 52(3-4): 839-850.
- https://doi.org/10.1016/j.ijheatmasstransfer.2008.07.032
 [3] Lareo, C.A., Fryer, P.J. (1998). Vertical flows of solid-
- liquid food mixtures. Journal of Food Engineering, 36(4): 417-443. https://doi.org/10.1016/S0260-8774(98)00066-1
- [4] Sandeep, K.P., Zuritz, C.A. (1995). Residence times of multiple particles in non-Newtonian holding tube flow: Effect of process parameters and development of dimensionless correlations. Journal of Food Engineering, 25(1): 31-44. https://doi.org/10.1016/0260-8774(95)93014-M
- [5] Sandeep, K.P., Zuritz, C.A., Puri, V.M. (2000). Modelling non-Newtonian two-phase flow in conventional and helical-holding tubes. International Journal of Food Science and Technology, 35(5): 511-522. https://doi.org/10.1046/j.1365-2621.2000.00408.x
- [6] Harimi, S., Marjani, A., Moradi, S. (2016). Numerical simulation of fluid flow and forced convection heat transfer around a circular cylinder with control rods located in equilateral triangular arrangement. Journal of Mechanical Science and Technology, 30(9): 4239-4246. https://doi.org/10.1007/s12206-016-0836-8
- [7] Chakraborty, J., Verma, N., Chhabra, R.P. (2004). Wall effects in flow past a circular cylinder in a plane channel: A numerical study. Chemical Engineering and Processing: Process Intensification, 43(12): 1529-1537. https://doi.org/10.1016/j.cep.2004.02.004
- [8] Paramane, S.B., Sharma, A. (2009). Numerical investigation of heat and fluid flow across a rotating circular cylinder maintained at constant temperature in 2-D laminar flow regime. International Journal of Heat and Mass Transfer, 52(13-14): 3205-3216. https://doi.org/10.1016/j.ijheatmasstransfer.2008.12.031
- [9] Aminossadati, S.M., Raisi, A., Ghasemi, B. (2011). Effects of magnetic field on nanofluid forced convection in a partially heated microchannel. International Journal of Non-Linear Mechanics, 46(10): 1373-1382. https://doi.org/10.1016/j.ijnonlinmec.2011.07.013
- [10] Singha, S., Sinhamahapatra, K.P. (2010). Flow past a circular cylinder between parallel walls at low Reynolds numbers. Ocean Engineering, 37(8-9): 757-769. https://doi.org/10.1016/j.oceaneng.2010.02.012
- [11] Rahim Mashaei, P., Hosseinalipour, S.M., Bahiraei, M. (2012). Numerical investigation of nanofluid forced convection in channels with discrete heat sources. Journal of Applied Mathematics, 2012(1): 259284. https://doi.org/10.1155/2012/259284
- [12] Fu, W.S., Tong, B.H. (2004). Numerical investigation of heat transfer characteristics of the heated blocks in the channel with a transversely oscillating cylinder. International Journal of Heat and Mass Transfer, 47(2):

- 341-351. https://doi.org/10.1016/S0017-9310(03)00303-x
- [13] Selimefendigil, F., Öztop, H.F. (2018). Magnetic field effects on the forced convection of CuO-water nanofluid flow in a channel with circular cylinders and thermal predictions using ANFIS. International Journal of Mechanical Sciences, 146: 9-24. https://doi.org/10.1016/j.ijmecsci.2018.07.011
- [14] Mohebbi, R., Rashidi, M.M., Izadi, M., Sidik, N.A.C., Xian, H.W. (2018). Forced convection of nanofluids in an extended surfaces channel using lattice Boltzmann method. International Journal of Heat and Mass Transfer, 117: 1291-1303. https://doi.org/10.1016/j.ijheatmasstransfer.2017.10.063
- [15] Zhang, M., Wang, X., Øiseth, O. (2021). Torsional vibration of a circular cylinder with an attached splitter plate in laminar flow. Ocean Engineering, 236: 109514. https://doi.org/10.1016/j.oceaneng.2021.109514
- [16] Al-Sumaily, G.F., Sheridan, J., Thompson, M.C. (2012). Analysis of forced convection heat transfer from a circular cylinder embedded in a porous medium. International Journal of Thermal Sciences, 51: 121-131. https://doi.org/10.1016/j.ijthermalsci.2011.08.018
- [17] Rashidi, S., Bovand, M., Esfahani, J.A. (2015). Heat transfer enhancement and pressure drop penalty in porous solar heat exchangers: A sensitivity analysis. Energy Conversion and Management, 103: 726-738. https://doi.org/10.1016/j.enconman.2015.07.019
- [18] Matin, M.H., Pop, I. (2013). Forced convection heat and mass transfer flow of a nanofluid through a porous channel with a first order chemical reaction on the wall. International Communications in Heat and Mass Transfer, 46: 134-141. https://doi.org/10.1016/j.icheatmasstransfer.2013.05.00
- [19] Al-Sumaily, G.F., Nakayama, A., Sheridan, J., Thompson, M.C. (2012). The effect of porous media particle size on forced convection from a circular cylinder without assuming local thermal equilibrium between phases. International Journal of Heat and Mass Transfer, 55(13-14): 3366-3378. https://doi.org/10.1016/j.ijheatmasstransfer.2012.03.007
- [20] Al-Sumaily, G.F., Thompson, M.C. (2013). Forced convection from a circular cylinder in pulsating flow with and without the presence of porous media. International Journal of Heat and Mass Transfer, 61: 226-244.
 - https://doi.org/10.1016/j.ijheatmasstransfer.2013.01.067
- [21] Kumar, A., Dhiman, A.K. (2012). Effect of a circular cylinder on separated forced convection at a backward-facing step. International Journal of Thermal Sciences, 52: 176-185. https://doi.org/10.1016/j.ijthermalsci.2011.09.014

NOMENCLATURE

Ср	specific heat at constant pressure, J/kg. K				
D	diameter of circular cylinder, m				
Da	Darcy number				
h	convection heat transfer coefficient	nt,			
	$W/(m^2.K)$				
K	thermal conductivity, W/(m. K)				
Nu	local Nusselt number				

\overline{Nu}	average Nusselt number	Greek symbol	S
p	PRESSURE, Pa		
p P	dimensional pressure	α	channel sides angle
Pr	Prandtl number	θ	dimensionless temperature
Re	Reynold number	φ	volume fraction
T	temperature, K	μ	dynamic viscosity, kg/(m. s)
U	dimensionless velocity component in X-	υ	kinematic viscosity of fluid, m ² /s
	direction	ρ	density, kg/m ³
V	dimensionless velocity component in Y-		
	direction	Subscripts	
X	non-dimensional coordinate in horizontal		
	direction	c	cold
Y	non-dimensional coordinate in vertical	f	fluid phase
	direction	h	hot
		nf	nanofluid